EFFECT OF RANDOM PARAMETERS IN SEMI-EMPIRICAL METHOD ON THE RESULTS OF GROUND MOTION PREDICTIONS

J. Miyakoshi[1], K. Dan[1], A. Fukukita[1] and A. Okazaki[2]

[1] *Shimizu Corporation, Tokyo, Japan*
[2] *Kansai Electric Power Company, Osaka, Japan*
Email: miyakoshi@shimz.co.jp , kazuo.dan@shimz.co.jp , fukukita@shimz.co.jp, okazaki.atsushi@e3.kepco.co.jp

ABSTRACT:
We examined the effects of the random parameters in the stochastic Green's function method on the predicted strong ground motions in this paper. Assuming lateral strike-slip faults, we changed the phase of the stochastic Green's functions and the location of the point source of the seismic wave, and evaluated the variation of the simulation results. We applied this procedure to the strike-slip fault models with the different positions of the hypocenters, with the different locations of the asperities, and with the different numbers of the asperities. The results of the simulation showed that the coefficient of variation of the peak ground accelerations and that of the peak ground velocities were about 20 – 40 % for each simulation model.

KEYWORDS:
random parameter, semi-empirical method, ground motion prediction, asperity model

1. INTRODUCTION

The ground motions are often predicted by a semi-empirical method (*e.g.*, Irikura, 1986; Takemura and Ikeura, 1987; Dan and Sato, 1998) in Japan. The semi-empirical method in cludes two methods: one is the empirical Green's function method using actual smaller size earthquake records as Green's functions and the other is the stochastic Green's function method using artificial waves generated in computers as Green's functions. When the ground motions are synthesized by the stochastic Green's function method (Dan *et al.*, 2005), we use two kinds of random parameters in this method. One is the random initial value of phase used in generating the stochastic Green's functions. The other is the random location of the point source inside each subfault that radiates seismic waves (Zhao *et al.*, 1995). However, examination about how these random parameters influence the predicted ground motions has not been performed.
Hence, in this study, we examined the effect of these random parameters on the predicted ground motions in the stochastic Green's function method. We simulated the strong ground motions for lateral strike-slip faults by changing these random parameters. In addition to these simulations, we also calculated the strong ground motions for the different positions of the hypocenter, the different locations of the asperity, and the different numbers of the asperities.

2. FAULT MODEL

We assumed lateral strike-slip models with a magnitude M_{JMA} of 6.8. Here, M_{JMA} is the Japan Meteorological Agency magnitude. The fault parameters were determined by the procedure of Irikura and Miyake (2001). Figure 1 shows an example of the faults, and Table 1 shows the fault parameters. The fault length was 23 km, the fault width was 17 km, the depth of the top of the fault was 3 km, and the ratio of the area of the asperity to the entire fault area (Sa/S) was 22 % (Somerville *et al.*, 1999). We calculated the strong ground motions at 13 points shown in Figure 2. We also calculated the strong ground motions for the fault models with the different positions of the hypocenters shown in Figure 1, with the different locations of the asperities shown in Figure 3, and with the different numbers of the asperities shown in Figure 4. We determined the position and the number of asperities from the inversion models of past earthquakes (*e.g.* Miyakoshi *et al.*, 2000). Table 2 summarizes the fault models and statistics we focused on.

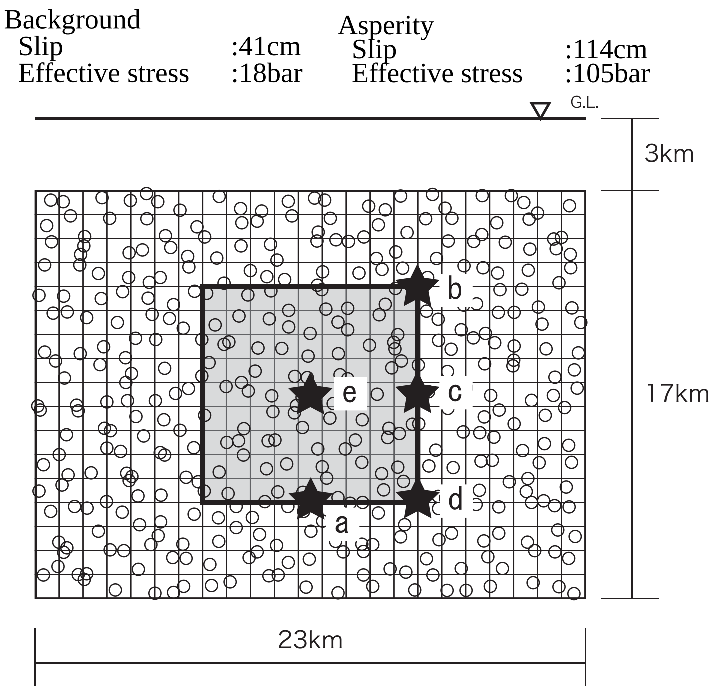

Figure 1 Fault model in case of varying the position of the hypocenter

Parameters	Value
Strike	N090E
Dip	90
Rake	0
M_{JMA}	6.8
M_W	6.5

Table 1 Fault parameters

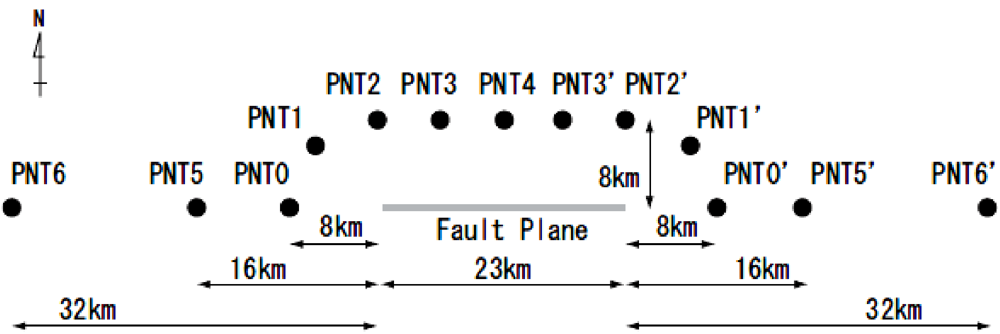

Figure 2 Calculation points

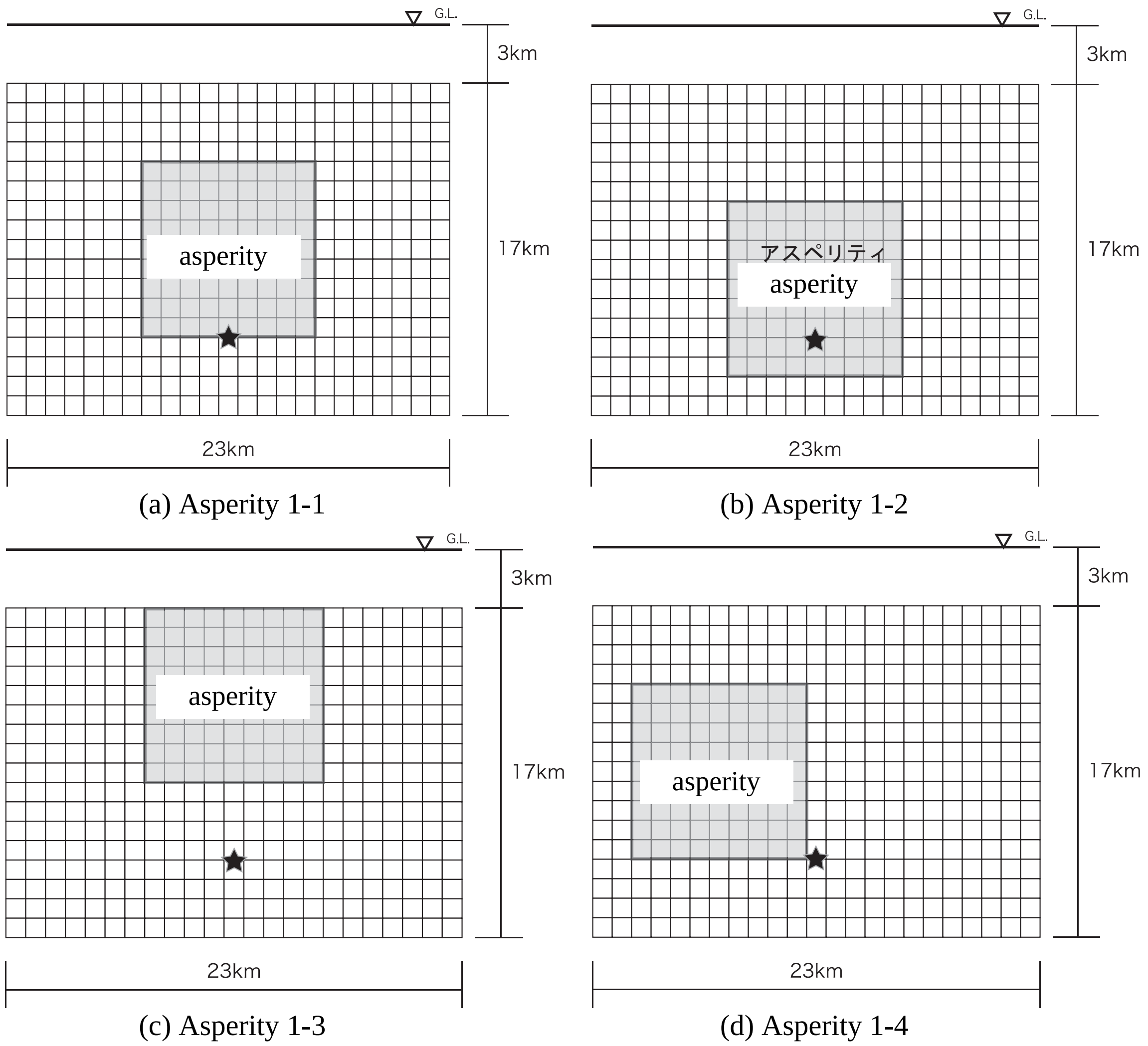

Figure 3 Fault models with different position of the asperity

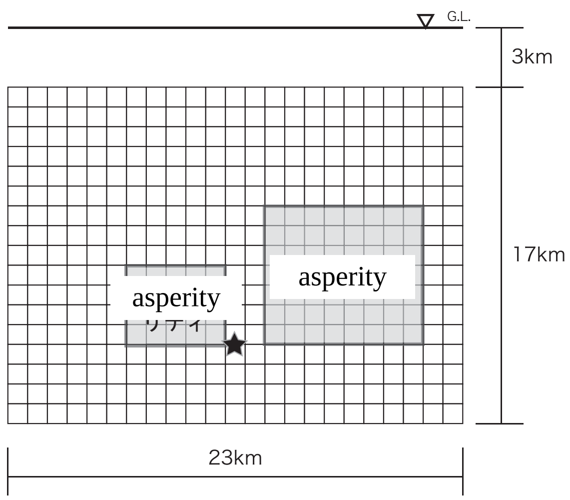

Figure 4 Fault model with two asperities (Asperity 2-1)

Table 2 Variation of fault models and evaluated statistics

Position and number of asperities	Hypocenter	Calculation points	Random variation	Physical index	Direction	Statistics
1-1	a b c d e	PNT0, 0' PNT1, 1' PNT2, 2' PNT3, 3' PNT4 PNT5, 5' PNT6, 6'	Phase: 100 × Location of point source of seismic wave: 100 ‖ 10,000	Acceleration Velocity Pseudo-velocity response spectrum	fault normal fault parallel	Average Standard deviation Coefficient of variation
1-2	a					
1-3	a					
1-4	a					
2-1	a					

3. SIMULATION RESULTS

3.1. Effect of Phases of Stochastic Green's Function

We calculated the strong ground motions in the fault-normal direction and the fault-parallel direction at each calculation point by the stochastic Green's function method. The stochastic Green's functions were generated with 100 kinds of initial values phases.

Figure 5 shows the probability density distribution of the peak ground accelerations (PGA) and the peak ground velocities (PGV) in the fault-normal direction at PNT0 for the fault model of asperity 1-1. Table 3 shows the average, the standard deviation, and the coefficient of variation (ratio of the standard deviation to the average) of the PGA and PGV in each direction at PNT0 for the fault model of asperity 1-1. The coefficients of variation of the PGA in the fault-normal and fault-parallel directions were 12 % and 14%, and the coefficients of variation of the PGV in the fault-normal and fault-parallel directions were 22 % and 14%. We adapted a log-normal distribution for the probability density functions of the PGA and the PGV shown in Figure 5. The probability density functions of the PGA and PGV at PNT0 were found to be modeled pretty well by the log-normal distribution. The results at the other calculation points were similar to the results at PNT0.

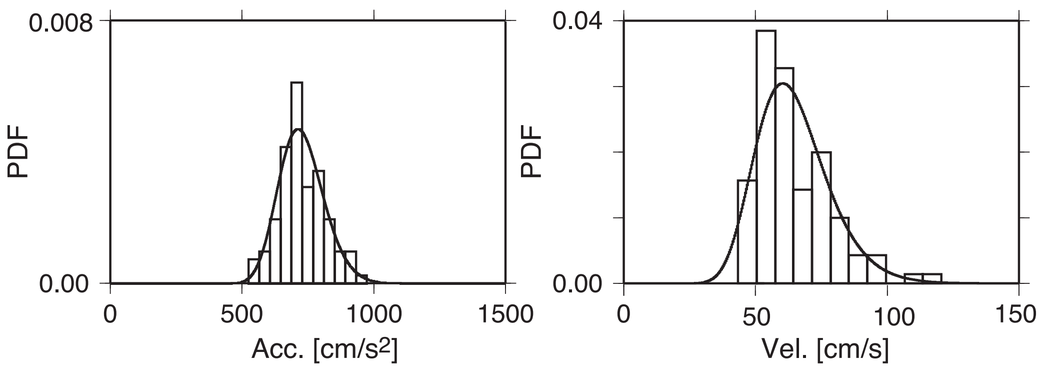

Figure 5 Distribution of the peak ground motions in the fault-normal direction in case of changing the phases of the stochastic Green's functions at PNTO with the fault model of asperity 1-1

Table 3 Average, standard deviation, and coefficient of variation of the peak ground accelerations and velocities in case of changing the phase of the stochastic Green's function at PNTO for the fault model of asperity 1-1

	Direction	Average	Standard deviation	Coefficient of variation
PGA (cm/s^2)	fault parallel	373	50.7	0.14
	fault normal	728	86.2	0.12
PGV (cm/s)	fault parallel	7.3	1.0	0.14
	fault normal	64.6	13.9	0.22

3.2. Effect of both Phases of Stochastic Green's Function and locations of Point Sources inside Subfaults

We calculated the strong ground motions by using not only the different phases of the stochastic Green's functions but also the different locations of the point sources of the seismic waves. We calculated totally 10,000 ground motions combined 100 kinds of the phases of the stochastic Green's functions and 100 kinds of the locations of the point sources. The example of the location of the point sources is shown by the circles in Figure 1.

Figure 6 shows the probability density functions of the PGA and PGV in the fault-normal direction at PNT0 for the fault model of asperity 1-1. Table 4 shows the average, the standard deviation, and the coefficient of variation of the PGA and PGV in each direction at PNT0 for the fault model of asperity 1-1. The coefficients of variation of the PGA and PGV in each direction were around 20 %. The average of the PGA and PGV differed in Table 3 and Table 4, in order that those averages changed according to the location of the point source.

Figure 7 shows the coefficients of variation of the PGA and PGV in each direction at each calculation point for the fault model of asperity 1-1. The coefficients of variation of the PGA in each direction at each calculation point were around 20 %. The coefficients of variation of the PGV depended on the direction and the calculation point, and were from 20 % to 40 %. When the average of the PGV was small because of the radiation pattern, the coefficients of variation of the PGV were lager than about 20 %.

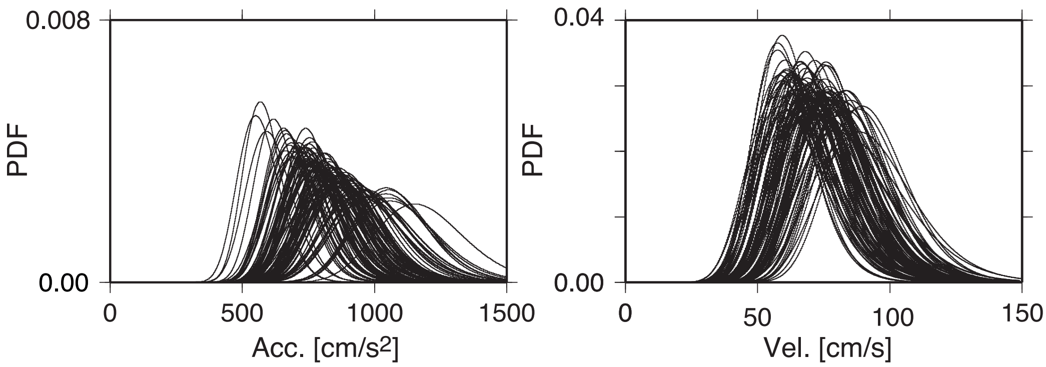

Figure 6 Distribution of the peak ground motions at PNTO in the fault-normal direction in case of changing both the phases of the stochastic Green's functions and the locations of the point sources on the subfault for the fault model of asperity 1-1, calculation point of PNT0)

Table 4 Average, standard deviation, and coefficient of variation of the peak ground accelerations and velocities in case of changing both the phases of the stochastic Green's functions and the locations of the point sources of the seismic waves at PNTO for the fault model of asperity 1-1

	Direction	Average	Standard deviation	Coefficient of variation
PGA (cm/s^2)	fault parallel	365	78.7	0.22
	fault normal	839	167	0.20
PGV (cm/s)	fault parallel	6.9	1.6	0.23
	fault normal	75.1	16.5	0.22

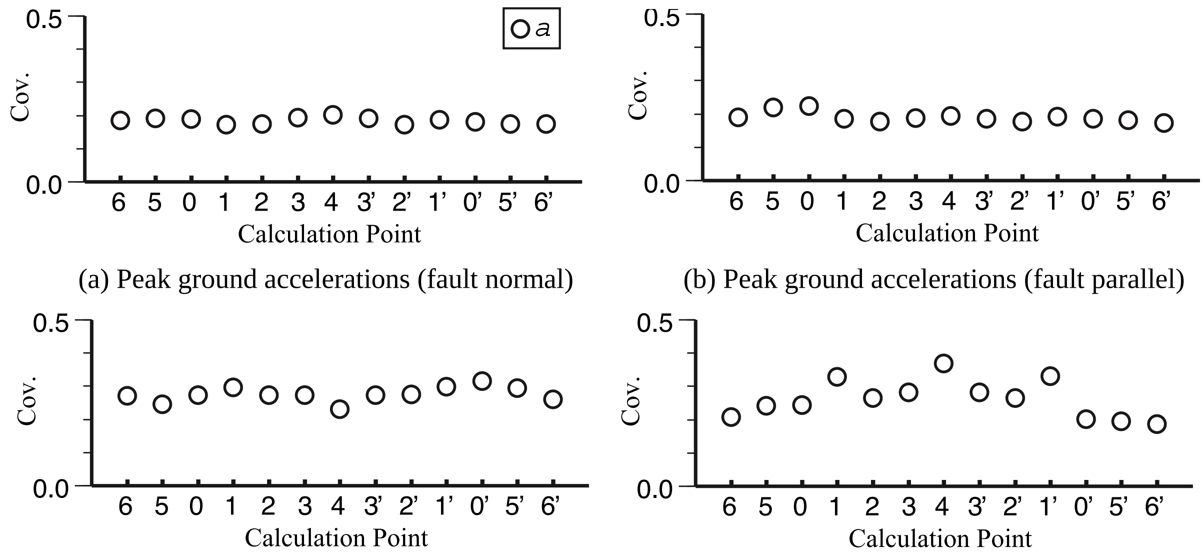

(a) Peak ground accelerations (fault normal) (b) Peak ground accelerations (fault parallel)

(c) Peak ground velocities (fault normal) (d) Peak ground velocities (fault parallel)

Figure 7 Coefficient of variation of the peak ground accelerations and velocities at each calculation point for the fault model of asperity 1-1

3.3. Effect of Positions of Hypocenters, locations of Asperities, and Number of Asperities

We calculated the strong ground motions for the fault models with the different positions of the hypocenters, with the different locations of the asperities, and with the difference numbers of the asperities.

Figure 8 shows the coefficients of variation of the PGA and PGV in each direction at each calculation point for the fault model with different positions of the hypocenters. Figure 9 shows the coefficients of variation of the PGA and PGV in each direction at each calculation point for the fault model with the different positions of the asperities and the difference numbers of the asperities. The coefficients of variation of the PGA in each direction at each calculation point were around 20 %. The coefficients of variation of the PGV depended not only on the direction and the calculation point but also on the position of the hypocenters, the position of the asperities, and the number of the asperities.

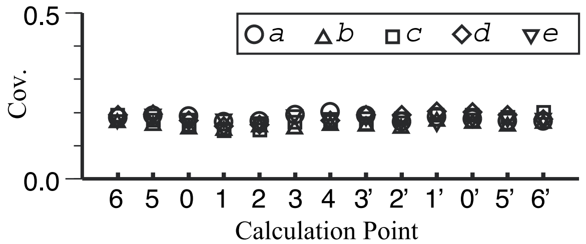

(a) Peak ground accelerations (fault normal)

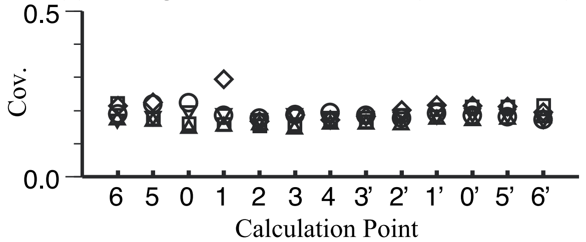

(b) Peak ground accelerations (fault parallel)

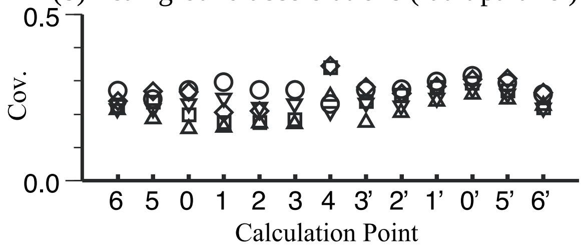

(c) Peak ground velocities (fault normal)

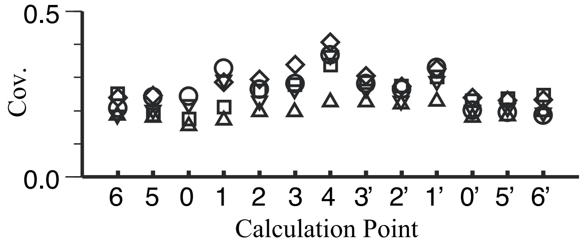

(d) Peak ground velocities (fault parallel)

Figure 8 Coefficient of variation of the peak ground accelerations and velocities at each calculation point in case of changing the positions of the hypocenters

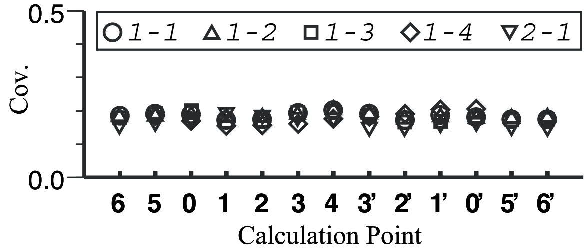

(a) Peak ground accelerations (fault normal)

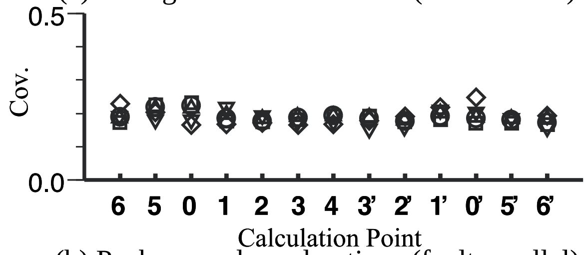

(b) Peak ground accelerations (fault parallel)

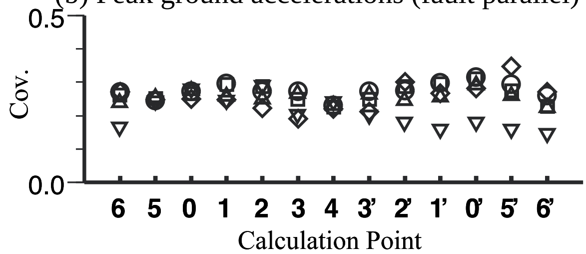

(c) Peak ground velocities (fault normal)

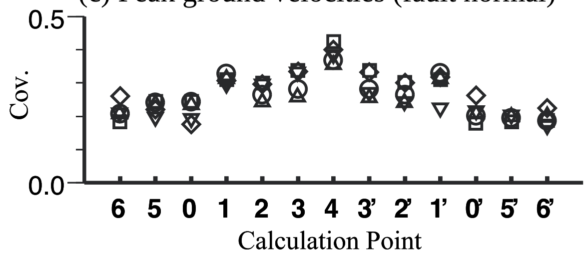

(d) Peak ground velocities (fault parallel)

Figure 9 Coefficient of variation of the peak ground accelerations and velocities at each calculation point in case of changing the position and the number of the asperities

4. CONCLUSIONS

We examined the effects of random parameters on the strong ground motions predicted by the stochastic Green's function method. Random parameters were the phases of the stochastic Green's functions and the locations of the point sources. We calculated 10,000 strong ground motions for lateral strike-slip faults changing these random parameters. In addition to these calculations, we also calculated the strong ground motions for the fault models with the different locations of the hypocenters, with the different locations of the asperities, and with the difference numbers of the asperities. For the results, the coefficients of variation of the peak ground accelerations were around 20%. Those of the peak ground velocities were from 20% to 40%, depending on the direction and the calculation point because of the radiation pattern.

ACKNOWLEDGMENTS

All the results in this paper were obtained in the research project by the group of Tokyo Electric Power Company and other 11 Japanese electric power companies.

REFERENCES

Dan, K. and Sato, T. (1998). Strong-motion prediction by semi-empirical method based on variable-slip rupture model of earthquake fault, *Journal of Structural and Construction Engineering* (*Transactions of Architectural Institute of Japan*) **509**, 49-60 (in Japanese).

Dan, K., Muto, T., Miyakoshi, J. and Watanabe, M. (2005). Estimation of effective stress on asperities in inland earthquakes caused by large strike-slip faults and its application to strong motion simulation, *Journal of Structural and Construction Engineering* (*Transactions of Architectural Institute of Japan*) **589**, 81-88 (in Japanese).

Irikura, K. (1986). Prediction of strong acceleration motions using empirical Green's function, *Proceedings of the Seventh Japan Earthquake Engineering Symposium*, 151-156.

Irikura, K. and Miyake, H. (2001). Prediction of strong ground motions for scenario earthquakes, *Journal of Geography* **110**, 849-875 (in Japanese).

Miyakoshi, K., Kagawa, T., Sekiguchi, H., Iwata, T. and Irikura, K. (2000). Source characterization of inland earthquakes in Japan using source inversion results, *Proceedings of the 12th World Conference on Earthquake Engineering* (CDROM).

Somerville, P., Irikura, K., Graves, R., Sawada, S., Wald, D., Abrahamson, N., Iwasaki, Y., Kagawa, T., Smith, N. and Kowada, A. (1999). Characterizing crustal earthquake slip models for the prediction of strong ground motion, *Seismological Research Letters* **70**, 59-80.

Takemura, M. and Ikeura, T. (1987). Semi-empirical synthesis of strong ground motions for the description of inhomogeneous faulting, *Journal of the Seismological Society of Japan Second Series* **59**, 77-80 (in Japanese).

Zhao, W., Dan, K. and Tanaka, T. (1995). Scaling factors in different semi-empirical methods for synthesizing earthquake motions, *Journal of Structural and Construction Engineering* (*Transactions of Architectural Institute of Japan*) **471**, 29-40 (in Japanese).